Доклади на Българската академия на науките
Comptes rendus de l'Académie bulgare des Sciences

Tome 77, No 5, 2024

GEOPHYSICS

Meteorology

DISTRIBUTION CHARACTERISTICS OF THE SHORT-TERM HEAVY RAINFALL OF AN MCC IN SHANDONG PROVINCE

Fujing Wan[1], Huaizhu Wang[2], Yi Zheng[3], Jianwei Yu[4]✉

Received on December 22, 2023
Presented by K. Stoykova, Corresponding Member of BAS, on March 26, 2024

Abstract

This study employs a comprehensive approach, utilizing conventional meteorological observation data, Fengyun satellite cloud imagery, and ERA5 reanalysis data to examine a short-term heavy rainfall event and its underlying causes in Shandong Province from August 14 to 16, 2020. The findings reveal that: (1) This event represents a typical Mesoscale Convective Complex (MCC)-induced rainfall process, with the primary precipitation zone in central and southern Shandong. The most intense hourly rainfall is observed along the side of the MCC with the steepest Tropical Brightness Temperature Blackbody (TBB) gradient. The heaviest hourly rainfall happens right around the time of the lowest TBB interval. (2) The rainfall event is marked by a vertical atmospheric structure with a high-altitude westerly jet and a low-level southwest jet, which makes it easy for water vapour to move and shear lines to form. Favourable conditions for water vapour convergence and high specific humidity are noted. During episodes of heavy precipitation, there is a marked upward motion in the lower troposphere, aligning with the vertical pattern of low-level convergence and high-level divergence.

Key words: short-time heavy precipitation, mesoscale convective complex, weather situation

This work was primarily supported by the National Natural Science Foundation of Shandong (Grants ZR2023MD118, ZR2021MD010, and ZR2021MD062), SDCXTD2023-1 and the Key Special Projects of Qingdao Meteorological Bureau (2023qdqxz02).

https://doi.org/10.7546/CRABS.2024.05.07

Introduction. The concept of a MCC was initially introduced by MADDOX in 1980 [1]. MCCs can trigger severe weather phenomena like flooding, damaging winds, and large hail [2–7]. These systems, notorious for causing short bursts of heavy rainfall, often lead to prolonged rainstorms and serious natural disasters. Forecasting and warning about such events, including MCCs, pose significant challenges [8–16]. Thus, studying the formation mechanisms, structural characteristics, large-scale circulation features, and cloud imagery of MCCs is crucial for accurate rainstorm forecasting. Research on MCCs has yielded numerous findings both domestically and internationally. BARTELS et al. [17] discovered a close correlation between the asymmetry of precipitation types, the three-dimensional flow field, and convective instability within MCCs. XI et al. [18] observed no significant correlation between precipitation intensity and maximum TBB values; however, they found a strong relationship between precipitation intensity and the TBB gradient in the northern part of the cloud cluster. JUNHONG et al. [19], through case studies, concluded that areas of heavy rainfall align with regions where the TBB in MCCs is $\leq -70\,^{\circ}\mathrm{C}$. Additionally, XIUGUANG et al. [20] identified that heavy rainfall areas are typically congruent with the western region of the TBB cold centre in cloud clusters.

In this article, the spatial distribution characteristics of heavy rainfall caused by MCC events and the causes of rainstorm are studied.

Data and physical-geographical factors. Time–space conversion of ordinary surface and upper-air observations, infrared brightness and microwave data from different satellites provided early insight into MCC. The data they also used included radars, aircraft instrumentation, satellite-borne radars, and high-resolution modelling in previous studies. In our studied area, the severe weather can be mainly divided into two categories: dry convection and wet convection. Dry type strong convection is mainly caused by thunderstorms, which are mainly influenced by the westerly belt system and caused by small-scale convective systems such as squall lines. Wet type severe convective weather is mainly characterized by heavy rainfall, which generally occurs at the edge of subtropical high-pressure systems. The atmosphere is rich in water vapour and is caused by mesoscale convective systems (MCS) or mesoscale convective complexes (MCC). The duration of maintenance is longer than the previous type and the range is also larger. Through synoptic analysis and dynamic diagnosis methods, an in-depth analysis is conducted focusing on the primary flood season in Shandong from August 14 to 16, 2020. The objective is to elucidate the distribution patterns of short-term heavy rainfall events caused by MCCs.

Weather process and disaster situation. The heavy rainfall event from August 14 to 16, 2020, was the only occurrence of an extremely intense rainstorm in August. This event was notable for its broad coverage, high intensity, prolonged duration, and complex causation. On August 14, the storm primarily affected south-central and southeastern Shandong, with 13 stations reporting

rainstorms. Yinan, Mengyin, and Linyi experienced exceptionally heavy downpours, accompanied by thunderstorm gusts ranging from 7 to 9. In Rizhao City, most areas experienced daily precipitation exceeding 50 mm, with some regions in Juxian County receiving over 100 mm. In Linyi City, the average daily precipitation reached 117.3 mm, with Yinan County recording an exceptional average of 264.6 mm. The peak hourly precipitation ranged between 50–70 mm.

Development and evolution of cloud and rain clusters. Analysis of hourly satellite cloud imagery reveals that the main precipitation cloud cluster formed over the Yellow Sea on the night of August 13 and began impacting southeastern Shandong on the 14th. The cloud cluster was roughly elliptical, with its long axis oriented east-west. By 4:00 on the 14th, the cloud cluster's structure began to loosen, with the area of the small TBB gradient in the northeast detaching at 7:00. The cluster then resumed an elliptical shape, with its major axis shifting to a northeast-southwest orientation, showing signs of weakening and dissipation. The cold centre's TBB intensity diminished, and the cold cloud area shrank. By approximately 11:00 on the 14th, the convective cloud cluster had largely dissipated. Concurrently, a smaller convective cloud cluster formed in central and southern Shandong and continued to develop. The area with TBB $\leq -63\,^{\circ}\mathrm{C}$ expanded westward, enlarging the cloud cluster. From 14:00 to 16:00, it merged with convective cloud clusters from southwestern Shandong and near the Yellow Sea (Fig. 1a), eventually reaching the scale of an MCC (Fig. 1b).

The period from 15:00 to 22:00 on August 14 was the peak developmental stage of the MCC. During this phase, the MCC maintained an approximately elliptical shape, with its long axis oriented east-west. The cloud cluster displayed a distinct Tropical Brightness TBB gradient, larger in the southwest and smaller in the northeast. The cold cloud cover area at $-52\,^{\circ}\mathrm{C}$ expanded, with the TBB in the cold centre remaining below $-63\,^{\circ}\mathrm{C}$ (Fig. 1d). Additionally, the formation of convective clouds with TBB intensities close to the main cluster in southwestern Shandong caused the MCC to extend southwestward. The movement of the entire system was relatively slow. An analysis of the maximum hourly rainfall locations and cloud cluster configurations revealed a substantial overlap between areas of high rainfall and high TBB gradients. Rainfall distribution was asymmetric, predominantly around the TBB cold centre and its southwestern side. After 12:00 on August 14, varied precipitation levels were observed in central and southern Shandong, with lower amounts in the central and eastern regions at this time. The peak period at this stage saw precipitation exceeding 50 mm at individual stations, corroborating the pattern of heavier rainfall in the west and lighter in the east. This phase, characterized by the most vigorous cloud cluster development, indicates that the peak of short-term heavy rainfall is driven by MCC activity.

By 23:00 on August 14, the MCC began to weaken. The area of cold clouds with TBB $\leq -63\,^{\circ}\mathrm{C}$ in the cold centre rapidly contracted, and the structure of the western cloud cluster started to disintegrate. The $-52\,^{\circ}\mathrm{C}$ cold cloud cluster tran-

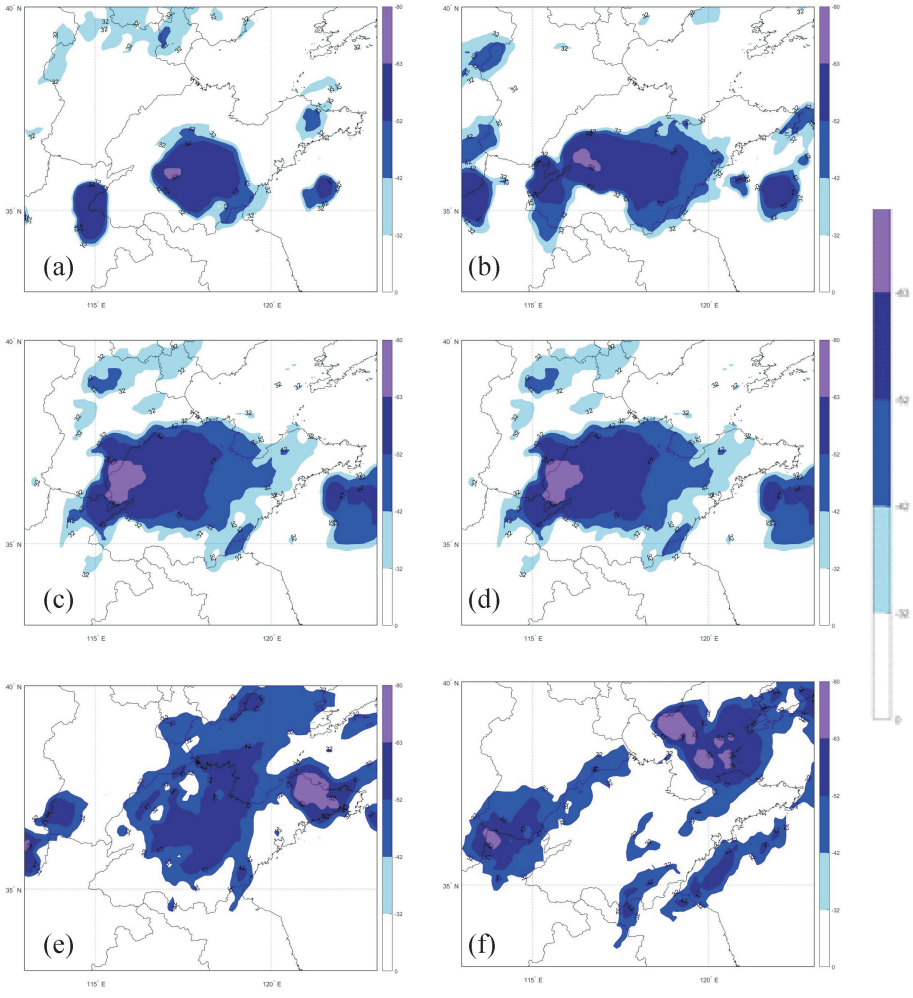


Fig. 1. Satellite cloud images of August 14–15, 2020 (a) 14:00, (b) 16:00, (c) 20:00, (d) 22:00, (e) 00:00, and (f) 05:00

sitioned from a unified to a fragmented structure, with its area also significantly decreasing. Nonetheless, the overall scale continued to meet the MCC criteria. On August 15, at 0:00, the structure became more dispersed, and the cloud cluster moved northeast under the influence of mid- to high-level winds (Fig. 1e). Precipitation significantly diminished during this stage. The main cloud cluster completely exited the Shandong region by 5:00 on August 15, losing its elliptical shape (Fig. 1f), marking the end of the MCC event.

On August 15th, multiple scattered, block-like convective clouds formed across Shandong throughout the day without merging. Influenced by mid- to high-level westerly winds, these clouds moved eastward towards the sea. High-altitude winds were guiding convective clouds that originated in Henan and Hebei

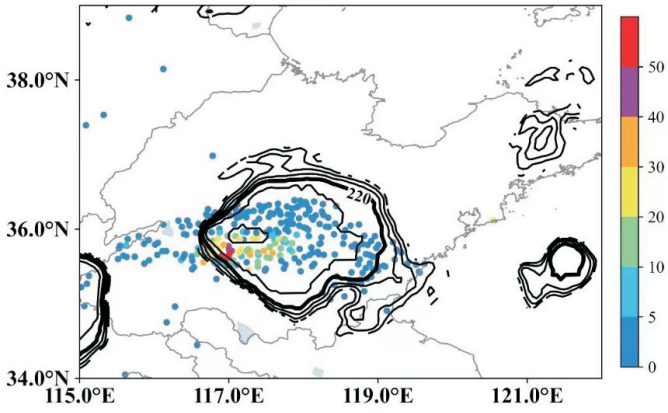


Fig. 2. Precipitation at 22:00 on August 14th (Scattered Points, Unit: mm) and Cloud TBB (Contour, Unit: K) Spatial distribution map, colour coded by precipitation size (e)

provinces as they passed through the northern part of Shandong. These convective systems did not significantly precipitate in the Shandong region. In conclusion, the relationship between cloud clusters and precipitation during this event is notable. Areas of high precipitation closely correspond with the development level of the MCC. The distribution of the strongest hourly precipitation during the peak activity of the MCC is asymmetric, characteristic of a typical MCC-induced precipitation process.

Analysis of large-scale circulation background. On the high-altitude 500 hPa map from August 14th, the atmospheric configuration in the mid- to high-latitude regions displayed a typical "two troughs and one ridge" pattern. The high-pressure ridge was situated south of the Central Siberian Mountains, with the Shandong region positioned downstream of the northeast cold vortex. The circulation pattern was relatively flat, placing Shandong on the right side of the entrance to the high-altitude westerly jet (Fig. 3a), experiencing positive vorticity advection. The westward extension and northward lifting tendencies of the West Pacific Subtropical High, coupled with the strengthening of the high-pressure centre, positioned Shandong at the edge of the subtropical high. The southwest airflow facilitated the transport of warm and humid air. This played a role in the region's cloud formation factors, along with the westerly jet's weak cold air.

The 700 hPa vortex exhibits a westward inclination relative to the 500 hPa vortex, and the temperature trough lags behind the height trough, leading to increased stratification instability (Fig. 3b). At the 850 hPa level, a southwest low-level jet stream is present in the southern part of the Shandong region. Additionally, a low-level shear line is observed in central and southern Shandong (Fig.

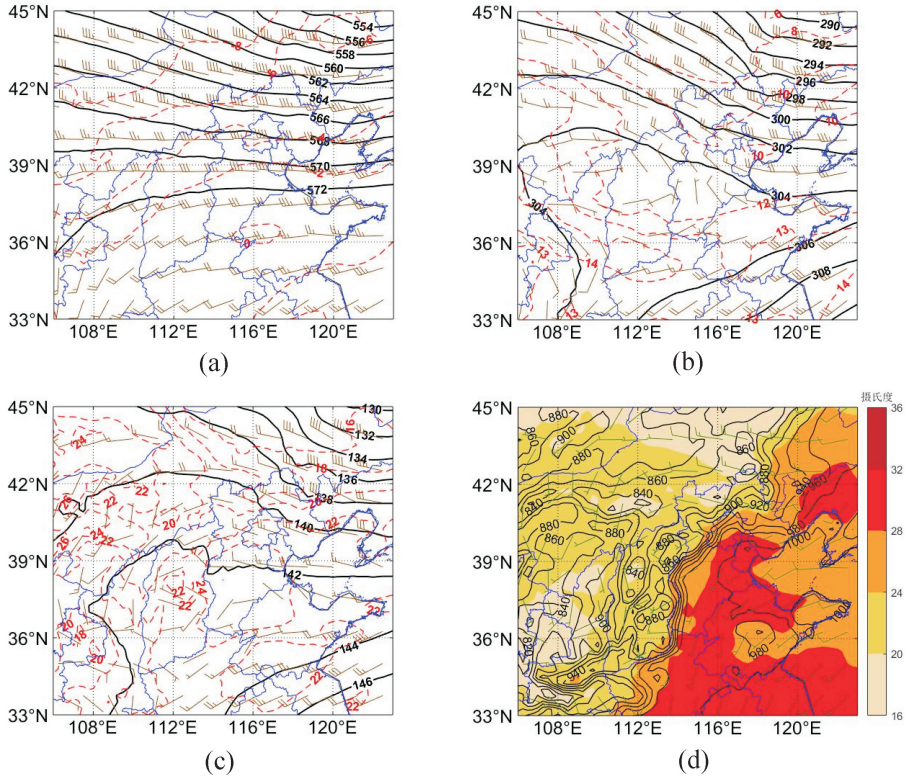


Fig. 3. Weather map at 500 hPa (a), 700 hPa (b), 850 hPa (c), and surface level (d) at 8:00 on August 14, 2020

3c), marked by pronounced horizontal convergence conducive to upward movement. The surface map reveals that, due to warm zone control at the 700 hPa and 850 hPa levels, the temperature distribution remains essentially unchanged (Fig. 3d).

Overall, throughout this weather event, the warm and humid airflow from the periphery of the West Pacific Subtropical High intersected with cold air from the base of the Northeast Cold Vortex in Shandong. The southwest low-level jet and low-level shear lines were the primary meteorological systems driving this precipitation event, with the southwest jet providing crucial water vapour conditions for rainfall.

Environmental field condition analysis. ***Water vapour conditions.*** For precipitation, the humidity in the lower atmosphere plays a crucial role. The advection of water vapour in the lower atmosphere can lead to a localized increase in specific humidity, creating conditions favourable for precipitation. At 8:00 on August 14, the specific humidity in the central and southern parts of Shandong Province reached 16 g/kg (Fig. 4a). By 20:00 on the same day, the 16 g/kg contour line showed a distinct northward shift under the influence of warm and humid air

transported by the southwest airflow. Other contour lines in the southwestern region of Shandong also exhibited an upward trend (Fig. 4b). This pattern is closely linked to where the low-level westerly jet is located. This is because moist advection causes the local specific humidity to rise, which creates the right conditions for precipitation to happen in the area.

Additionally, if the effects of evaporation and turbulent transport from the underlying surface are disregarded under certain conditions, the water vapour equation can be considered a secondary term. When combined with the continuity equation and integrated across the entire atmosphere, the calculation formula is as follows:

$$\frac{1}{g}\int_0^{p0}\frac{\partial q}{\partial t}dp+\frac{1}{g}\int_0^{p0}grad(Vq)dp=-M. \tag{1}$$

In this equation, $M=\frac{1}{g}\int_0^{p0}cdp$ represents the atmospheric condensation value per unit area, meaning precipitation (atmospheric condensation value) equals the sum of atmospheric water vapour flux convergence and local water vapour variation. Considering the minimal contribution of water vapour in the upper atmosphere, only the troposphere is factored in. Given that the specific humidity in the storm area shows little temporal variation, the first term is disregarded. Consequently, the convergence balance of near-surface water vapour flux equates to precipitation.

The precipitation within the entire rainstorm area is not solely attributed to the convergence of water vapour flux. This convergence within the rainstorm zone inevitably causes water vapour from the surrounding areas to flow towards the storm centre. The divergence field in the peripheral regions directs this influx of moisture into the rain area. However, the precipitation within an area during a rain event is a result of both the local convergence flux of water vapour and the larger-scale convergence field of water vapour flux in the surrounding areas. Additionally, the loss of water vapour in the outer area needs replenishment to sustain the rainstorm. Therefore, for a rainstorm process, the water vapour flux convergence field must be large-scale, characterized by water vapour convergence in the rain area, divergence in the outer area, and overall convergence in the outer area.

Thermal conditions. The thermodynamic characteristics of the atmosphere are crucial for understanding rainstorm dynamics and should be necessarily analyzed from various perspectives, including Convective Available Potential Energy (CAPE), atmospheric unstable stratification, and the K index. In the warm season, convective weather in the Shandong region typically exhibits an average CAPE below 500, along with a K index around 26 °C. The distribution of CAPE is characterized by higher values on the flanks and lower values in the middle. The highest CAPE, located in the southern part of Hebei Province and the central

and southern regions of Shandong Province, reaches a maximum of 2000 J/kg. By 5:00 p.m. on the day following the end of the MCC, high CAPE values had moved away from the Shandong Peninsula. The CAPE across the entire Shandong region dropped below 1000 J/kg, signalling a reduction in the intensity of the precipitation. In some areas, CAPE fell to less than 500 J/kg, making the maintenance of heavy rainfall challenging. Consequently, the precipitation focus began shifting from the entire Shandong region to specific local areas within the province.

Moreover, the K index serves as a scalar for analyzing atmospheric stability, with its value inversely related to stability levels. At 20:00 on August 14, the high-value area, located in central and southern Shandong and peaking over 40 °C, was in the southwestern region of Shandong Province. This indicates a high degree of atmospheric instability, conducive to triggering large-scale thunderstorm processes.

Lifting conditions. For rainfall to occur, a strong upward motion zone in the precipitation area is necessary, along with an appropriate divergence field.

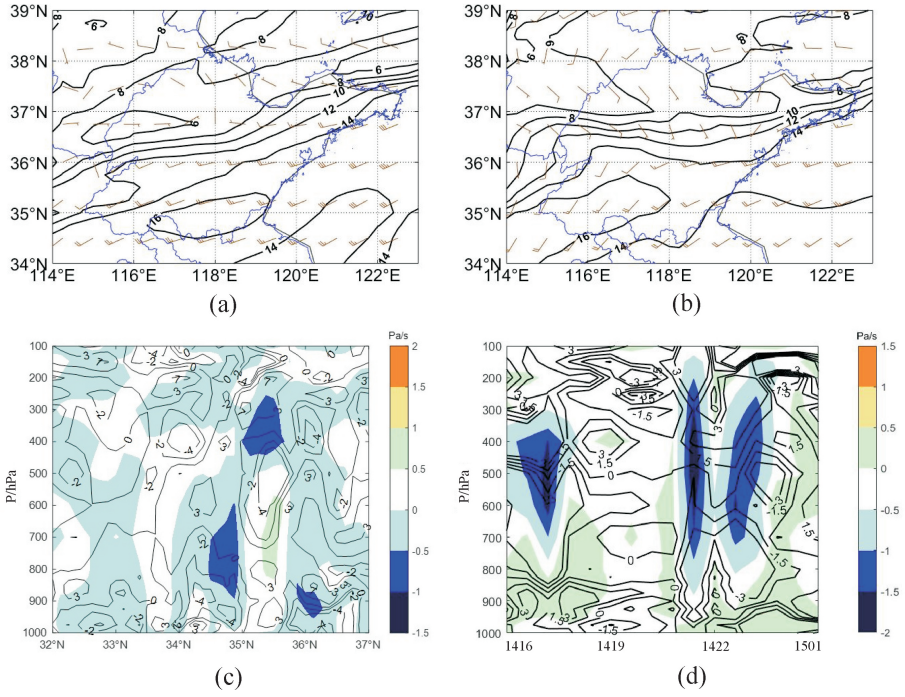


Fig. 4. Specific humidity (Isoline, Unit: g/kg) and Wind field distribution at 850 hPa at 8:00 (a) and 20:00 (b), (c) Longitudinal profile of vertical velocity and divergence at 22:00 on August 14, 2020, (d) Time profile of vertical velocity and divergence in Mengyin (Colouring: Vertical velocity, Unit: Pa/s, Contour line: Divergence, Unit: 10^{-5}m/s)

Given the high precipitation intensity near 116.75° E, the longitudinal profile of vertical velocity and divergence at 22:00 on August 14, using 116.75° E as a reference, is illustrated in Fig. 4c. A significant upward motion zone is observed between 34° N and 35° N, with a central intensity around 1 Pa/s. The conversion relationship between Pa/s and m/s is established by the ideal gas state equation ($PM = \rho RT$) and $\omega = -\rho gw$, where ρ represents air density, M is the gas molar mass, T is temperature, and g is gravitational acceleration. The numerical conversion relationship between the two is qualitatively negative, predominantly located around 600–850 hPa. This rising range aligns with previous analyses in central and southern Shandong Province. Divergence centres near 300 hPa in the upper layer are present alongside numerous convergence centres around 850 hPa near 34.5° N. Moderate convergence is observed from 500 hPa to 700 hPa in the middle layer. The spatial distribution of vertical velocity is well-matched with the divergence field. The effective coordination between lower-level convergence, upper-level divergence, and the ascending motion area guarantees dynamic conditions conducive to vigorous rainstorm activity.

Additionally, considering the significant development of the MCC during the rainy season in Mengyin County, an analysis of the time profile of vertical velocity and divergence fields near Mengyin County, Linyi City (Fig. 4d), reveals a deep vertical velocity zone around 20:00 to 22:00 on August 14, with a central intensity of about 2 Pa/s, spanning from 200 hPa to 800 hPa. The divergence field also displays a reasonable configuration. This phase corresponds to a period of intense local precipitation and the peak of MCC development. This suggests that that a strong upward movement combined with an appropriate divergence field provides dynamic environmental conditions favourable for rainstorm development and precipitation intensification.

Other conditions. The undulating terrain of mountains in North China makes certain areas, particularly the mountains and their windward sides, prone to rainstorms. This is primarily due to forced terrain uplift and systematic changes in wind direction across the terrain, leading to convergence or divergence in certain areas. Furthermore, the terrain can alter the clouds' micro-physical state, enhancing the conversion of condensed water into rainfall. A line chart based on 36° N latitude, detailing the changes in altitude and precipitation from 20:00 to 3:00 on August 14th, reveals that lower latitude wind directions in the Shandong region move from west to east. Higher precipitation values are predominantly found on the windward slopes of mountain ranges, aligning with sea-level elevation trends. This suggests that terrain features significantly impact precipitation distribution and intensity.

Conclusion. The entire precipitation event can be categorized into three distinct phases. The warm, humid air from the Western Pacific Subtropical High, which the low-level jet and low-level vortex shear intensified, was the cause of the rainfall that hit southeastern Shandong before 8:00 a.m. on April 14. The

MCC, which developed at 3:00 p.m. on the 14th, dictated the precipitation in central southern and northeastern Shandong from 12:00 p.m. to 5:00 p.m.. During this phase, the areas of highest precipitation largely coincided with the high Tropical Brightness TBB gradient areas of the MCC, predominantly located in the southwest region of the cloud cluster, exhibiting typical MCC precipitation characteristics. The short-term precipitation in northern Shandong around 8:00 on the 16th is directly linked to the heavy rainfall in southern Hebei Province.

The peak of short-term heavy rainfall occurred in central and southern Shandong, marked by increased specific humidity and water vapour convergence. Surrounding the rainfall area, there was significant water vapour convergence, fulfilling the necessary conditions for precipitation. At the same time, a strong link was seen between low-level convergence and high-level divergence in central and southern Shandong. This created dynamic conditions for the start and continuation of precipitation. The entire short-term heavy rainfall process was characterized by an initial increase in convective available potential energy in central and southern Shandong, followed by a decline towards the precipitation's end. The short-term heavy rainfall in Shandong showed positive feedback to terrain effects, with a marked increase in precipitation in mountainous areas and windward slopes. This research work can provide useful reference for MCC rainstorm precipitation forecast in warm season in Huang Huai region. The use of MCC cloud map features can accurately determine the precipitation area of heavy rainfall and offer scientific, accurate, and timely short-term forecasts for flood control departments.

REFERENCES

[1] Maddox R. A. (1983) Large-scale meteorological conditions associated with midlatitude, mesoscale convective complexes, Monthly Weather Review, **111**(7), 1475–1493.

[2] Shaowen S., L. Shenshen, Y. Xiuping (2009) Mesoscale Meteorology, Beijing Meteorological Publishing House, 320–421.

[3] Min S., D. Jianhua, Y. Zhaohong, T. Lan (2015) An analysis of a back-propagating thunderstorm using the three-dimensional wind fields retrieved by the dual-Doppler radar data, Acta Meteorologica Sinica, **2**, 247–262.

[4] Jinglin L. H., W. Zhikai (2020) Causation Analysis of a Strong Squall Line Storm in Northeast Sichuan on April 9 in 2019, Desert and Oasis Meteorology, **14**(4), 52–60.

[5] Wan F., S. Jisong, S. Min, M. Chanjuan (2021) Impacts of sea breeze front over Shandong Peninsula on the evolution of a squall line, Acta Meteorologica Sinica, **79**(5), 717–731.

[6] Changyi X., Z. Lina, X. Xian et al. (2023) Case analysis of damaging high winds generated by bow echoes in the presence of a cold vortex over the North China Plain, Acta Meteorologica Sinica, **81**(1), 40–57.

[7] Zhongping D., M. Zhan Yun (2021) Analysis of radar echoes and wind profiles of four squall lines in Jiangxi Province, Desert and Oasis Meteorology, **15**(6), 75–82.

[8] Yongguang Z., T. Zuyu, W. Hongqing et al. (2002) The Yellow Sea and surrounding areas, the environmental conditions under which mesoscale convective systems occur, Journal of Meteorology, **3**(5), 613–619.
[9] Maoqiang C., G. Qingyuan, W. Yanbo (2008) Characteristics of mesoscale convective cloud clusters of a southwest vortex extremely heavy rainstorm, Research on Plateau Mountain Meteorology, **28**(4), 66–71.
[10] Fujing W., D. Xiuguang (2018) Analysis of Differences and Similarities between Two MCC Infrared Cloud Images and Weather Conditions, Meteorology, **44**(6), 759–770.
[11] Yunyun Y., L. Hongwu, S. Tao et al. (2021) Analysis of a Heavy Rainfall Weather Process in Hunan, Meteorological Technology, **49**(3), 446–454.
[12] Li R., Y. Yanmin (2021) Analysis of dynamic and thermal characteristics of a MCC rainstorm at the bottom of the northeast cold vortex, Drought Meteorology, **39**(1), 65–86.
[13] Velasco I., J. M. Fritsch (1987) Mesoscale convective complexes in the Americas, Journal of Geophysical Research: Atmospheres, **92**(D8), 9591–9613.
[14] Maddox R. A. (1980) Mesoscale convective complexes, Bulletion of the American Meteorological Society, **61**(11), 1374–1387.
[15] Fang Z. (1985) The preliminary study of medium-scale cloud clusters over the Changjiang basin in summer, Advances in Atmospheric Sciences, **2**(3), 334–340.
[16] Benxiang Y., T. Zuyu (2005) The analysis of local features of MCC on southeast Tibetan plateau, Acta Meteorologica Sinica, **2**, 236–242.
[17] Bartels D. L., R. A. Maddox (1991) Midlevel cyclonic vortices generated by mesoscale convective systems, Monthly Weather Review, **119**(1), 104–118.
[18] Xi J., G. Qingyun, Y. Jing et al. (2011) Comparative analysis of MCC with two different precipitation magnitudes, Plateau Meteorology, **30**(2), 328–338.
[19] Junhong F., W. Xinpu, M. Kai (2009) Cloud map characteristics and genesis analysis of an MCC, Plateau Meteorology, **28**(6), 1388–1398.
[20] Xiuguang D., M. Xiangui, W. Mingbo (2015) Evolution characteristics and genesis analysis of a MCC infrared cloud map, Shandong Meteorology, **35**(2), 1–7.

[1]*Qingdao Meteorological Bureau, Qingdao 266003, China*
e-mail: 1005418392@qq.com

[2]*Qcean University of China, Qingdao 266003, China*
e-mail: min_angela@126.com

[3]*Shandong Meteorological Bureau, Jinan 250000, China*
e-mail: zhengyi_316@163.com

[4]*Jiangsu Meteorological Bureau, Nanjing 210000, China*
e-mail: radargroup@foxmail.com